Nonsingular Fast Terminal Sliding Mode Control Based on Nonlinear Disturbance Observer for a Quadrotor

ZHAO Jing[1,2*], *WANG Peng*[1,2], *SUN Yanfei*[1,2], *XU Fengyu*[1,2], *XIE Fei*[3,4]

1. College of Automation & College of Artificial Intelligence, Nanjing University of Posts and Telecommunications, Nanjing 210023, P. R. China;
2. Jiangsu Engineering Lab for IOT Intelligent Robots, Nanjing University of Posts and Telecommunications, Nanjing 210023, P. R. China;
3. School of Electrical and Automation Engineering, Nanjing Normal University, Nanjing 210023, P.R. China;
4. Nanjing Zhongke Raycham Laser Technology Co., Ltd., Nanjing 210023, P.R. China

(Received 23 June 2020; revised 1 November 2020; accepted 5 January 2021)

Abstract: Given external disturbances and system uncertainties, a nonsingular fast terminal sliding mode control (NFTSMC) method integrated a nonlinear disturbance observer (NDO) is put forward for quadrotor aircraft. First, a NDO is proposed to estimate the actual values of uncertainties and disturbances. Second, the NFTSM controller based on the reaching law is designed for the attitude subsystem (inner loop), and the control strategy can ensure Euler angles' fast convergence and stability of the attitude subsystem. Moreover, the NFTSMC strategy combined with backstepping is proposed for the position subsystem (outer loop), which can ensure subsystem tracking performance. Finally, comparative simulations show the trajectory tracking performance of the proposed method is superior to that of the traditional sliding mode control (SMC) and the SM integral backstepping control under uncertainties and disturbances.

Key words: quadrotor aircraft; nonlinear disturbance observer (NDO); nonsingular fast terminal sliding mode control (NFTSMC); disturbances

CLC number: TP273, V279, V249.1 **Document code:** A **Article ID:** 1005-1120(2022)02-0219-12

0 Introduction

During the past decade, quadrotor unmanned aerial vehicles (UAVs) have attracted extensive research interest of many scientists all over the world. Compared with conventional aircraft, the quadrotors have many unique advantages, such as low cost, easy operation, hover control and so on. Therefore, the quadrotors are used to accomplish various tasks, such as military surveillance, agricultural investigation, and payload transport[1-4]. In practice, they are susceptible to external disturbances, which is easy to cause a relatively large discrepancy in attitude calculations. Consequently, the effective control is bound to decrease. Therefore, the influence of external disturbances on flight control stability should be concerned and solved in the design of controllers.

Various advanced control methods are proposed not only to stabilize the control system but also to improve system tracking performance, such as backstepping control[5], sliding mode control (SMC)[6-8], adaptive control[9], fuzzy control[10], etc. As we all know, SMC is regarded as an effective technique that results in a high degree of robustness to tackle system uncertainties and external disturbances. Mu et al.[11] studied an integral SMC to weaken the impact on the bounded external disturbances and model uncertainties. Wang et al.[12] used a terminal SMC strategy for controlling the quadcopter rotation and translation subsystem considering external distur-

*Corresponding author, E-mail address: zhaojing@njupt.edu.cn.

How to cite this article: ZHAO Jing, WANG Peng, SUN Yanfei, et al. Nonsingular fast terminal sliding mode control based on nonlinear disturbance observer for a quadrotor[J]. Transactions of Nanjing University of Aeronautics and Astronautics, 2022, 39(2): 219-230.

http://dx.doi.org/10.16356/j.1005-1120.2022.02.008

bances. A hierarchical SMC strategy was proposed to copy with continuous disturbance and parameter uncertainty by Li et al[13]. Zhang et al.[14] designed an improved robust controller for the sliding mode and the controller not only stabilized the quadcopter system, but also performed well against time-varying disturbances.

However, the above approaches only utilize the robustness of SMC to tackle system uncertainties and unknown external disturbances. To improve robustness, an observer is usually used to suppress and compensate for unknown system uncertainties and external disturbances. For example, Nuradeen et al.[15] used a method—combining SMC with a robust disturbance observer to stabilize the system and track the command trajectory. Additionally, Shi et al.[16] proposed an attenuation-control strategy based on a generalized extended state observer, which can meet the high-precision control target. Benallegue et al.[17] presented a high-order SMC based on disturbance observer strategy that is capable of dealing the effect of external disturbances.

Further, the backstepping technology is excellent for dealing with under-actuated nonlinear systems. Due to the under-actuated subsystem in the quadrotor system, the backstepping technology is widely adopted in the design of controllers. Chen et al. [18] applied the backstepping technology to the quadrotor position loop. Shao et al.[19] studied a stable trajectory tracking strategy combining the extended state and the backstepping technology to tackle the quadrotor system involving external disturbances and parameter uncertainties. Djamel et al.[20] designed an optimal control method for a quadrotor's attitude control based on the backstepping and nonlinear approach.

Inspired by the above approaches, we propose a nonsingular fast terminal sliding mode control (NFTSMC) combined with a nonlinear disturbance observe (NDO) for a quadrotor subjected to system uncertainties and external disturbances. The main innovations of this paper are summarized as follows:

(1) The designed observer can efficiently estimate the actual values of compound unknown disturbances. Compared with Ref.[21], it does not require the condition that the time derivative of the disturbance needs to be close to zero.

(2) Compared with the sliding mode control integral backstepping (IBS-SMC)[22], the classical SMC[23], the proposed NFTSM controller shows great advantages on a quadrotor system, such as accurate tracking performance, fast convergence and ability of avoiding the singularity problems.

(3) The robustness of a quadrotor system is strong by introducing NDO design. Meanwhile, Gaussian white noises can be effectively suppressed.

The rest of the paper is organized as follows. The disturbed model of quadrotors is introduced in Section 1. Then, NDO is used to estimate the uncertainties and disturbances in Section 2. Further, a backstepping NFTSMC based on the reaching law for the attitude and the position subsystems is constructed in Section 3. Some contrast results are shown in Section 4. Finally, some conclusions are drawn in Section 5.

1 Problem Formulation

1.1 Dynamic model of quadrotors

The structure of a quadrotor is illustrated in Fig.1. Let us employ two reference frames: The axes of the inertial coordinate are denoted as (O_e, x_e, y_e, z_e) and the axes of the body coordinate are denoted as (O_b, x_b, y_b, z_b). The vector $\boldsymbol{\eta}=[x, y, z]^{\mathrm{T}}$ denotes the position subsystem in the inertial coordinate. The vector $\boldsymbol{\xi}=[\phi, \theta, \psi]^{\mathrm{T}}$ expresses Euler angles in the inertial coordinate and the three Euler angles are roll $(-\pi/2<\phi<\pi/2)$ rad, pitch $(-\pi/2<\theta<\pi/2)$ rad and yaw $(-\pi<\psi<\pi)$ rad.

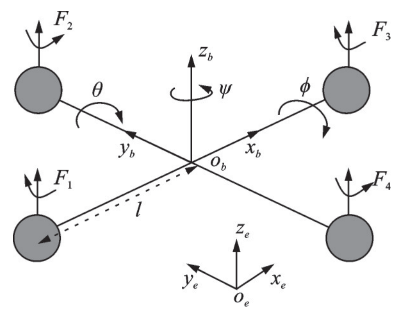

Fig.1 A quadrotor's structure

The vector $\boldsymbol{\omega}=[p, q, r]^{\mathrm{T}}$ denotes the angular velocities in the body coordinate, that is, roll, pitch, and yaw, respectively.

The dynamic model of a quadrotor is described in the form[19]

$$\begin{cases} \ddot{\phi}=a_1\dot{\theta}\dot{\psi}-a_2\dot{\phi}+U_1 \\ \ddot{\theta}=a_3\dot{\phi}\dot{\psi}-a_4\dot{\theta}+U_2 \\ \ddot{\psi}=a_5\dot{\theta}\dot{\phi}-a_6\dot{\psi}+U_3 \\ \ddot{x}=\left(C_\phi S_\theta C_\psi+S_\phi S_\psi\right)U_4-a_7\dot{x} \\ \ddot{y}=\left(C_\phi S_\theta C_\psi-S_\phi S_\psi\right)U_4-a_8\dot{y} \\ \ddot{z}=C_\phi C_\theta U_4-g-a_9\dot{z} \end{cases} \tag{1}$$

where g is the gravitational force; U_1, U_2, and U_3 represent the control input for the three attitude angle channels, U_4 is the control input for the position subsystem, and U_1, U_2, U_3, U_4 satisfy the relationships as follows

$$U_1=l\kappa(\Omega_4^2-\Omega_2^2)/I_x$$
$$U_2=l\kappa(\Omega_3^2-\Omega_1^2)/I_y$$
$$U_3=l\kappa(\Omega_2^2+\Omega_4^2-\Omega_1^2-\Omega_3^2)/I_z$$
$$U_4=l\kappa(\Omega_1^2+\Omega_2^2+\Omega_3^2+\Omega_4^2)/m$$

where $\Omega_i(i=1,2,3,4)$ is the speed of the ith rotor; $\boldsymbol{I}=\mathrm{diag}(I_x, I_y, I_z)$ denotes the moment of the inertial. $a_i(i=1,\cdots,9)$ in Eq.(1) is some known constants, and their detailed expressions are as follows

$$a_1=\frac{I_y-I_x}{I_x},\ a_2=\frac{J_\phi}{I_x}, a_3=\frac{I_z-I_x}{I_y}$$
$$a_4=\frac{J_\theta}{I_y}, a_5=\frac{I_x-I_y}{I_z}, a_6=\frac{J_\psi}{I_z}$$
$$a_7=\frac{J_x}{m}, a_8=\frac{J_y}{m}, a_9=\frac{J_z}{m}$$

where m is the total mass of a quadrotor; J_ϕ, J_θ, J_ψ, J_x, J_y and J_z are corresponding drag coefficients.

1.2 Disturbed quadrotor dynamic model

Considering system's uncertainties and external disturbances as an integration item, we name d_i, d_j. Eq.(1) can be decomposed into the following forms

$$\begin{cases} \dot{X}_{1i}=X_{2i} \\ \dot{X}_{2i}=f\left(X_{2i}\right)+U_i+d_i \\ \dot{X}_{1j}=X_{2j} \\ \dot{X}_{2j}=f\left(X_{2j}\right)+V_j+d_j \end{cases} \tag{2}$$

where $i=1,2,3$; $j=4,5,6$.

$$\begin{bmatrix} X_{11} \\ X_{12} \\ X_{13} \end{bmatrix}=\begin{bmatrix} \phi \\ \theta \\ \psi \end{bmatrix} \qquad \begin{bmatrix} X_{14} \\ X_{15} \\ X_{16} \end{bmatrix}=\begin{bmatrix} x \\ y \\ z \end{bmatrix}$$

$$\begin{bmatrix} V_4 \\ V_5 \\ V_6 \end{bmatrix}=\begin{bmatrix} U_x \\ U_y \\ U_z \end{bmatrix}=\begin{bmatrix} \left(C_\phi S_\theta C_\psi+S_\phi S_\psi\right)U_4 \\ \left(C_\phi S_\theta C_\psi-S_\phi S_\psi\right)U_4 \\ C_\phi C_\theta U_4 \end{bmatrix}$$

$f\left(X_{2i}\right)$ and $f\left(X_{2j}\right)$ are nonlinear terms, and the concrete expressions are as follows

$$\begin{bmatrix} f\left(X_{21}\right) \\ f\left(X_{22}\right) \\ f\left(X_{23}\right) \end{bmatrix}=\begin{bmatrix} a_1\dot{\theta}\dot{\psi}-a_2\dot{\phi} \\ a_3\dot{\phi}\dot{\psi}-a_4\dot{\theta} \\ a_5\dot{\theta}\dot{\phi}-a_6\dot{\psi} \end{bmatrix}$$

$$\begin{bmatrix} f\left(X_{24}\right) \\ f\left(X_{25}\right) \\ f\left(X_{26}\right) \end{bmatrix}=\begin{bmatrix} -a_7\dot{x} \\ -a_8\dot{y} \\ -g-a_9\dot{z} \end{bmatrix}$$

Assumption 1 For each subsystem, the lumped uncertainties d_i d_j are not measurable and unknown, and differentiable with bounded derivatives, i. e.

$$|\dot{d}_i|\leqslant D_i\ ,\ |\dot{d}_j|\leqslant D_j, t>0$$

For some positive constants D_i, D_j, $i=1,2,3, j=4,5,6$.

Remark 1 The disturbance for the system cannot be infinite, which means that the disturbance is bounded. It is unreasonable to only consider the constant disturbance in the system, that is, the derivative of the disturbance converges to zero, so the bounded derivative of the external disturbance is logical and reasonable[15].

1.3 Control strategy

The main control objectives of this paper are to design a control strategy combining NFTSMC and NDO, which can ensure the stability and tracking performance of a quadrotor system subjected to system uncertainties and external disturbances. A NDO is utilized to estimate lumped uncertainty, which compensate for lumped uncertainty. Then, via dividing a quadrotor system into two subsystems: Attitude and position, the controllers of the two subsystems are given. Based on that, the precise tracking and stability of the system are realized. The control diagram is shown in Fig.2.

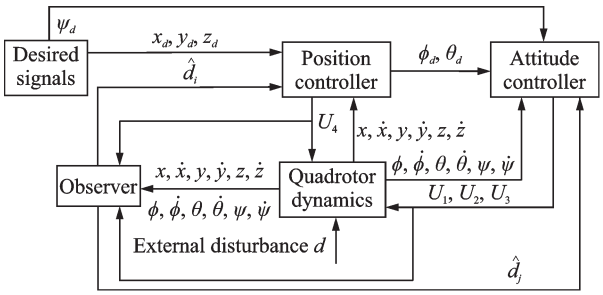

Fig.2 Control block diagram

2 Nonlinear Disturbance Observer Design

In this section, a NDO is designed to estimate the actual value of the lumped uncertainty. For both subsystems of the position and the attitude, NDO can take the same form

$$\begin{cases} \dot{Z}_i = -L_i Z_i - L_i\left[L_i X_{2i} + f\left(X_{2i}\right) + U_i\right] \\ \hat{d}_i = Z_i + L_i X_{2i} \\ \dot{Z}_j = -L_j Z_j - L_j\left[L_j X_{2j} + f\left(X_{2j}\right) + V_j\right] \\ \hat{d}_j = Z_j + L_j X_{2j} \end{cases} \tag{3}$$

where Z_i, Z_j are the states of NDO; L_i, L_j the observer gains; and $\hat{d}_i, \hat{d}_j$ the estimation of lumped uncertainties.

Define the estimation errors of NDO as

$$\tilde{d}_i = \hat{d}_i - d_i \tag{4}$$

Substituting Eqs.(2—4) into the derivative of $\hat{d}_i$, we obtain

$$\begin{aligned} \dot{\hat{d}}_i &= \dot{Z}_i + L_i \dot{X}_{2i} = \\ &-L_i \dot{Z}_i - L_i\left[L_i X_{2i} + f\left(X_{2i}\right) + U_i\right] + L_i \dot{X}_{2i} = \\ &-L_i\left(\dot{Z}_i + L_i X_{2i}\right) + L_i d_i = -L_i\left(\hat{d}_i - d_i\right) = \\ &-L_i \tilde{d}_i \end{aligned} \tag{5}$$

Then, the derivative of $\tilde{d}_i$

$$\dot{\tilde{d}}_i = -L_i \tilde{d}_i - \dot{d}_i \tag{6}$$

Hence, we obtain

$$\dot{\tilde{d}}_j = -L_j \tilde{d}_j - \dot{d}_j \tag{7}$$

Lemma 1 For smooth multivariate dynamic systems, V is assumed to be a strictly positive and continuously differentiable Lyapunov function. Let $C \subset \mathbf{R}^n$ be an arbitrarily given set of initial conditions for a connected and compact dynamic system. Further, suppose that along the trajectory system of any system, $x: \mathbf{R}^+ \to \mathbf{R}^n$, starting at C, differential inequality

$$\dot{V}\left(x(t)\right) < -\vartheta V\left(x(t)\right) + \omega$$

for all $t > 0$ with $x(0) \in C$ is satisfied with $\omega > 0$, a fixed positive constant, and ϑ, a positive and tunable parameter. In a sufficiently large time, all trajectories of the dynamic system are bounded starting in C for a sufficiently large time[15].

Theorem 1 If the system (2) satisfies Assumption 1, the observer gains L_i, L_j are selected as appropriate positive numbers. The disturbance estimations $\hat{d}_i$ $\hat{d}_j$ of Eq.(3) can asymptotically track the actual lumped uncertainties d_i, d_j of the system[21].

Proof Select the first Lyapunov candidate function as follows

$$V_{d_i} = \sum_{i=1}^{3} \frac{1}{2} \tilde{d}_i^2 \tag{8}$$

Taking the derivative of Eq.(8), we obatain

$$\begin{aligned} \dot{V}_{d_i} &= \sum_{i=0}^{3} \tilde{d}_i \dot{\tilde{d}}_i = \sum_{i=0}^{3} \tilde{d}_i\left(-L_i \tilde{d}_i - \dot{d}_i\right) = \\ &\sum_{i=0}^{3}(-L_i \tilde{d}_i^2 - \tilde{d}_i \dot{d}_i) \leqslant \\ &\sum_{i=0}^{3} -L_i \tilde{d}_i^2 + \frac{1}{2}\tilde{d}_i^2 + \frac{1}{2}\dot{d}_i^2 \leqslant \\ &\sum_{i=0}^{3} -\left(L_i - \frac{1}{2}\right)\tilde{d}_i^2 + \frac{1}{2}D_i^2 < \\ &\sum_{i=0}^{3} -\left(L_i - \frac{1}{2}\right)\tilde{d}_i^2 + D_i^2 \end{aligned} \tag{9}$$

Similarly, one obtains

$$\dot{V}_{d_j} < \sum_{i=0}^{3} -(L_j - \frac{1}{2})\tilde{d}_j^2 + D_j^2 \tag{10}$$

According to Lemma 1, the proof of Theorem 1 has been finished.

3 Controller Design

In this section, to control the system better, the double loop control method is adopted to deal with the underactuated property.

3.1 Attitude subsystem controller design

The NFTSMC method is proposed owing to its advantage of fast convergence of Euler angles. Firstly, attitude tracking errors are defined as follows: $e_1=\phi-\phi_d, e_2=\theta-\theta_d, e_3=\psi-\psi_d$. The NFTSM surface is designed as

$$s_i=e_i+\lambda_i\left|\dot{e}_i\right|^{\gamma}\operatorname{sgn}(\dot{e}_i) \tag{11}$$

where $i=1,2,3$; $\lambda_i>0$; $1<\gamma<2$.

An improved double power reaching law is proposed as

$$_{\Delta}\dot{s}_i=\frac{-2k_1}{1+e_i^{-c_1\Delta}}\left|s_i\right|^{\alpha}\operatorname{sgn}(s_i)+\frac{-2k_2e_i^{-c_2\Delta}}{1+e_i^{-c_2\Delta}}\left|s_i\right|^{\beta}\operatorname{sgn}(s_i) \tag{12}$$

where $\Delta=\left|s_i\right|-1$, $\alpha>1$, $0<\beta<1$, $k_1>0$, $k_2>0$, $c_1>0$ and $c_2>0$. Then the control laws are given by Eqs.(13—15).

$$U_1=\left[\frac{-2k_1}{1+e_1^{-c_1\Delta}}\left|s_1\right|^{\alpha}\operatorname{sgn}(s_1)+\frac{-2k_2e_1^{-c_2\Delta}}{1+e_1^{-c_2\Delta}}\left|s_1\right|^{\beta}\operatorname{sgn}(s_1)-\dot{e}_1\right]\frac{1}{\lambda_1\gamma}\left|\dot{e}_1\right|^{(1-\gamma)}-a_1\dot{\theta}\dot{\psi}+a_2\dot{\phi}+\ddot{\phi}_d-\rho_1s_1-\hat{d}_1 \tag{13}$$

$$U_2=\left[\frac{-2k_1}{1+e_2^{-c_1\Delta}}\left|s_2\right|^{\alpha}\operatorname{sgn}(s_2)+\frac{-2k_2e_2^{-c_2\Delta}}{1+e_2^{-c_2\Delta}}\left|s_2\right|^{\beta}\operatorname{sgn}(s_2)-\dot{e}_2\right]\frac{1}{\lambda_2\gamma}\left|\dot{e}_2\right|^{(1-\gamma)}-a_3\dot{\phi}\dot{\psi}+a_4\dot{\theta}+\ddot{\theta}_d-\rho_2s_2-\hat{d}_2 \tag{14}$$

$$U_3=\left[\frac{-2k_1}{1+e_3^{-c_1\Delta}}\left|s_3\right|^{\alpha}\operatorname{sgn}(s_3)+\frac{-2k_2e_3^{-c_2\Delta}}{1+e_3^{-c_2\Delta}}\left|s_3\right|^{\beta}\operatorname{sgn}(s_3)-\dot{e}_3\right]\frac{1}{\lambda_3\gamma}\left|\dot{e}_3\right|^{(1-\gamma)}-a_5\dot{\theta}\dot{\phi}+a_6\dot{\psi}+\ddot{\psi}_d-\rho_3s_3-\hat{d}_3 \tag{15}$$

Theorem 2 Given the lumped uncertainty in the attitude subsystem, if NFTSM controllers (13—15) are applied to system (2) under Assumption 1, the closed loop subsystem could guarantee the fast convergence and the stability.

Proof The roll angle is taken as an example, and the lumped uncertainty is d_1. The Lyapunov function is designed as

$$V_1=\frac{1}{2}s_1^2+V_{d_1} \tag{16}$$

Substituting Eq.(16) into the derivative of V_1, we obtain

$$\dot{V}_1=s_1\dot{s}_1+\dot{V}_{d_1}=s_1\Big(\dot{e}_1+\lambda_1\gamma\left|\dot{e}_1\right|^{(\gamma-1)}\Big(a_1\dot{\theta}\dot{\psi}-a_2\dot{\phi}+U_1-d_1-\ddot{\phi}_d\Big)\Big)+\tilde{d}_1\dot{\tilde{d}}_1\leqslant \frac{-2k_1}{1+e_1^{-c_1\Delta}}\left|s_1\right|^{(\alpha+1)}+\frac{-2k_2e_1^{-c_2\Delta}}{1+e_1^{-c_2\Delta}}\left|s_1\right|^{(\beta+1)}-\rho_1s_1^2-\left(L_1-\frac{1}{2}\right)\tilde{d}_1^2+\frac{1}{2}D_1^2<-\rho_1s_1^2-\left(L_1-\frac{1}{2}\right)\tilde{d}_1^2+\frac{1}{2}D_1^2<-\delta_1V_1+D_1^2 \tag{17}$$

where $\delta_1=\min\{2\rho_1,2L_1-1\}$.

The result of Theorem 2 comes from Lemma 1. Therefore, the control laws (13—15) are designed to ensure tracking performance of the attitude subsystem.

3.2 Position subsystem controller design

A backstepping NFTSM scheme is proposed for the position subsystem in this section. Here we take x position as an example to introduce the design process.

The position tracking error is

$$\varepsilon_1=x-x_d \tag{18}$$

The time derivative of x and it follows that

$$\dot{\varepsilon}_1=\dot{x}-\dot{x}_d=\alpha_1-\dot{x}_d \tag{19}$$

where α_1 is a virtual control input.

The first Lyapunov function is defined as

$$V_2=\frac{1}{2}\varepsilon_1^2 \tag{20}$$

The derivative of V_2 is as follows

$$\dot{V}_2=\varepsilon_1\dot{\varepsilon}_1=\varepsilon_1\left(\alpha_1-\dot{x}_d\right) \tag{21}$$

α_1 is designed as

$$\alpha_1=s_4-c\varepsilon_1+\dot{x}_d \tag{22}$$

where s_4 denotes the sliding surface and c is a constant.

Then, the NFTSM surface s_4 is designed as

$$s_4=\varepsilon_1+v_1\left|\varepsilon_1\right|^{p}\operatorname{sgn}(\varepsilon_1)+v_2\left|\dot{\varepsilon}_1\right|^{q}\operatorname{sgn}(\dot{\varepsilon}_1) \tag{23}$$

where v_1, v_2 are positive constants, and p, q ($q<p$) the positive odd numbers.

The time derivative of Eq.(23) follows that

$$\dot{s}_4=\dot{\varepsilon}_1+v_1p\left|\varepsilon_1\right|^{p-1}\dot{\varepsilon}_1+v_2q\left|\dot{\varepsilon}_1\right|^{q-1}(\ddot{x}-\ddot{x}_d) \tag{24}$$

The second Lyapunov function is defined as

$$V_3=V_2+\frac{1}{2}s_4^2 \tag{25}$$

The derivative of Eq.(25) obtains

$$\dot{V}_3 = \dot{V}_2 + s_4\dot{s}_4 = -c\varepsilon_1^2 + s_4\varepsilon_1 + s_4\left[\dot{\varepsilon}_1 + v_1 p\left|\varepsilon_1\right|^{p-1}\dot{\varepsilon}_1 + v_2 q\left|\dot{\varepsilon}_1\right|^{q-1}(\ddot{x} - \ddot{x}_d)\right] \tag{26}$$

By substituting Eq.(3) in Eq.(26), we get

$$\dot{V}_3 = -c\varepsilon_1^2 + s_4\varepsilon_1 + s_4\left[\dot{\varepsilon}_1 + v_1 p\left|\varepsilon_1\right|^{p-1}\dot{\varepsilon}_1 + v_2 q\left|\dot{\varepsilon}_1\right|^{q-1}(U_x - a_7\dot{x} + d_4 - \ddot{x}_d)\right] \tag{27}$$

The virtual control input U_x can be defined as

$$U_x = \left(-\varepsilon_1 - \dot{\varepsilon}_1 - v_1 p\left|\varepsilon_1\right|^{p-1}\dot{\varepsilon}_1\right)\frac{1}{v_2 q}\left|\dot{\varepsilon}_1\right|^{(1-q)} - \tau_1 s_4 + a_7\dot{x} - \hat{d}_4 + \ddot{x}_d \tag{28}$$

Similarly, the y, z position tracking errors are defined as

$$\varepsilon_2 = y - y_d \tag{29}$$

$$\varepsilon_3 = z - z_d \tag{30}$$

Virtual control inputs α_2, α_3 are designed as

$$\alpha_2 = s_5 - c\varepsilon_2 + \dot{y}_d \tag{31}$$

$$\alpha_3 = s_6 - c\varepsilon_3 + \dot{z}_d \tag{32}$$

And the sliding surface s_5, s_6 are defined as

$$s_5 = \varepsilon_2 + v_3\left|\varepsilon_2\right|^p \operatorname{sgn}(\varepsilon_2) + v_4\left|\dot{\varepsilon}_2\right|^q \operatorname{sgn}(\dot{\varepsilon}_2) \tag{33}$$

$$s_6 = \varepsilon_3 + v_5\left|\varepsilon_3\right|^p \operatorname{sgn}(\varepsilon_3) + v_6\left|\dot{\varepsilon}_3\right|^q \operatorname{sgn}(\dot{\varepsilon}_3) \tag{34}$$

The virtual control input U_y, U_z can be defined as

$$U_y = \left(-\varepsilon_2 - \dot{\varepsilon}_3 - v_3 p\left|\varepsilon_2\right|^{p-1}\dot{\varepsilon}_2\right)\frac{1}{v_4 q}\left|\dot{\varepsilon}_2\right|^{1-q} - \tau_2 s_5 + a_8\dot{y} - \hat{d}_5 + \ddot{y}_d \tag{35}$$

$$U_z = \left(-\varepsilon_3 - \dot{\varepsilon}_3 - v_5 p\left|\varepsilon_3\right|^{p-1}\dot{\varepsilon}_3\right)\frac{1}{v_6 q}\left|\dot{\varepsilon}_3\right|^{1-q} - \tau_3 s_6 + a_9\dot{z} + g - \hat{d}_6 + \ddot{z}_d \tag{36}$$

Theorem 3 For the quadrotor's position subsystem (2), given the design of NFTSM surface (23) combined with the backstepping technology and the estimated value of the lumped uncertainty obtained from observer (3), the designed control laws (28, 35, 36) can stabilize the position subsystem.

Proof Take x position for an example. The lumped uncertainty is denoted as d_4 and we select the Lyapunov function

$$V_4 = V_3 + \dot{V}_{d_4} \tag{37}$$

Substituting Eq.(27) into the derivative of $\dot{V}_4$, we obtain

$$\begin{aligned}\dot{V}_4 &= \dot{V}_3 + \tilde{d}_4\dot{\tilde{d}}_4 = -c\varepsilon_1^2 + s_4\varepsilon_1 + s_4\left[\dot{\varepsilon}_1 + v_1 p\left|\varepsilon_1\right|^{(p-1)}\dot{\varepsilon}_1 + v_2 q\left|\dot{\varepsilon}_1\right|^{(q-1)}(U_x - a_7\dot{x} + d_4 - \ddot{x}_d)\right] + \tilde{d}_4\dot{\tilde{d}}_4 = -c\varepsilon_1^2 - \tau_1 s_4^2 + \\ &\quad \tilde{d}_4\dot{\tilde{d}}_4 \leqslant -c\varepsilon_1^2 - \tau_1 s_4^2 - \left(L_4 - \frac{1}{2}\right)\tilde{d}_4^2 + \frac{1}{2}D_4^2 < -\delta_4 V_4 + D_4^2\end{aligned} \tag{38}$$

where $\delta_4 = \min\{2c, 2\tau_1, 2L_4 - 1\}$.

Similarly, the result of Theorem 3 can be obtained from Lemma 1. Therefore, the stability and tracking performance of the position subsystem are ensured under the control laws (28, 35, 36).

As mentioned above, the yaw angle ψ could track the given desired value ψ_d based on the attitude controllers. Therefore, θ_d, ϕ_d and U_4 can be calculated from Eqs.(28, 35, 36) with the ψ considered as known. The solutions are as follows

$$\begin{cases} U_4 = \sqrt{U_x^2 + U_y^2 + U_z^2} \\ \phi_d = \arcsin\left(\dfrac{U_x\sin\psi_d - U_y\cos\psi_d}{\sqrt{U_x^2 + U_y^2 + U_z^2}}\right) \\ \theta_d = \arctan\left(\dfrac{U_x\cos\psi_d + U_y\sin\psi_d}{U_z}\right) \end{cases} \tag{39}$$

Remark 2 It is worth noting that the yaw command ψ_d should satisfy $\psi_d \in (-\pi/2, \pi/2)$, such that the solvability of U_4 is guaranteed. Further, the condition also accords with the range of a yaw angle in practice.

Remark 3 To reduce the chatting characteristic of SMC, we substitute sat(s) for sgn(s) in this paper. The sat(s) function is defined as follows

$$\operatorname{sat}(s) = \begin{cases} \operatorname{sgn}(s) & |s| \geqslant \Delta \\ \dfrac{s}{\Delta} & |s| < \Delta \end{cases}$$

where Δ is a positive constant.

4 Simulation and Discussion

4.1 Parameter selection

To fully verify the efficiency and superiority of the proposed control technology, the closed-loop quadrotor system under NFTSMC controllers (13—15) and (28, 35, 36) and Eq.(3) are tested by simulations.

Quadrotor parameters The physical parameters of a quadrotor are chosen in Table 1.

Observer parameters The nonlinear observer gains are chosen as: $L_i = L_j = 15(i=1,2,3;\ j=4,5,6)$.

Controller parameters The attitude subsystem: $\lambda_i = 0.000\,1$, $\gamma = 1.1$, $\alpha = 1.02$, $\beta = 0.9$, $k_1 = 1.5$, $k_2 = 1.2$, $c_1 = 1.2$, $c_2 = 1.4$, $\rho_1 = \rho_2 = \rho_2 = 5$; the position subsystem: $c = 3$, $p = 5$, $q = 3$, $v_1 = v_3 = v_5 = 20$, $v_2 = v_4 = v_6 = 5$, $\tau_1 = \tau_2 = \tau_3 = 5$.

Table 1 Parameter setting of quadrotors

Symbol	Value	Symbol	Value
m/kg	2	I_x, I_y/ $(\mathrm{N \cdot s^2 \cdot rad^{-1}})$	1.25
l/m	0.2	I_z/ $(\mathrm{N \cdot s^2 \cdot rad^{-1}})$	2.5
$\tau/(\mathrm{N \cdot s^2 \cdot rad^{-2}})$	1.15×10^{-7}	J_x, J_y, J_z/ $(\mathrm{N \cdot s \cdot rad^{-1}})$	0.01
$\kappa/(\mathrm{N \cdot s^2 \cdot rad^{-2}})$	2.98×10^{-6}	J_ϕ, J_θ, J_ψ/ $(\mathrm{N \cdot s \cdot rad^{-1}})$	0.012

4.2 Simulation results

The desired position trajectory is set as

$$[x_d, y_d, z_d] = [\sin t,\ \cos t, 3t]\,\mathrm{m}$$

The desired signal of the yaw angle is set as $\psi_d = \frac{\pi}{3}$ rad, and the initial states are $x_0 = y_0 = z_0 = 0$ m, $\phi_0 = \theta_0 = \psi_0 = 0$. The objective of the simulation results is to compare and confirm the advantages of the proposed approach compared with the different approaches. Three simulation scenarios will be set to verify the effectiveness of the algorithm.

4.2.1 Scenario 1: Trajectory tracking under ideal case

In this scenario, we focus on the stability and performance of the proposed strategy without disturbances. To demonstrate the capabilities of the provided controllers, they were compared with SM integral backstepping control[23] (IBS-SMC) and conventional SMC[24] (SMC) approaches.

The tracking responses of attitude angles in Scenario 1 are presented in Fig. 3, and the actual yaw angle is nearly fully tracked the desired signal. Here, the NFTSMC is compared with IBS-SMC and SMC approaches. According to Fig.3, IBS-SMC and SMC performance is worse than that of the NFTSMC. Further, Fig.4 shows that the tracking errors of the attitude subsystem in NFTSMC are relatively smaller than that in IBS-SMC and SMC.

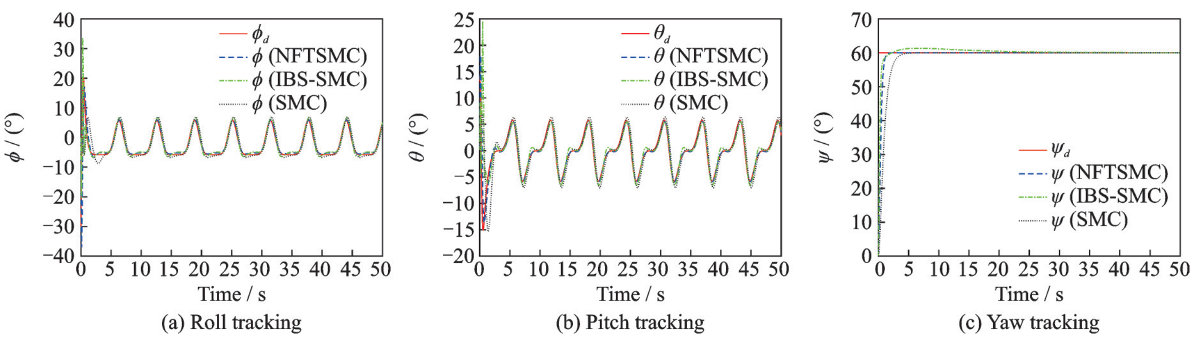

(a) Roll tracking (b) Pitch tracking (c) Yaw tracking

Fig.3 Attitude tracking in Scenario 1

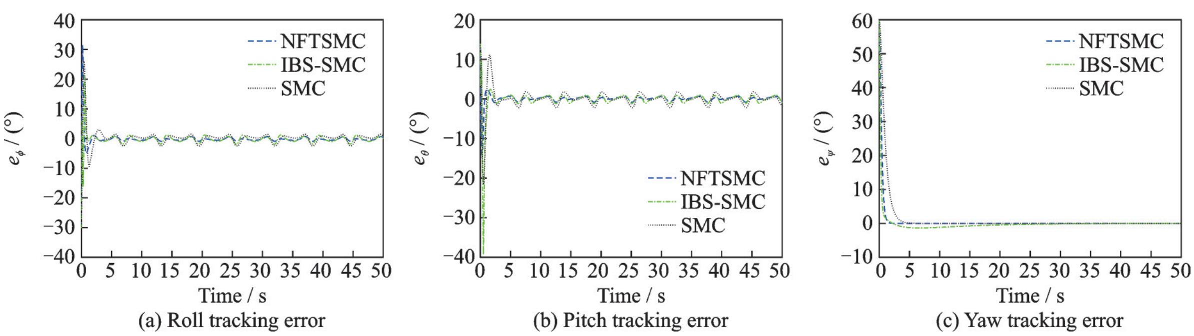

(a) Roll tracking error (b) Pitch tracking error (c) Yaw tracking error

Fig.4 Attitude tracking errors in Scenario 1

In Scenario 1, for the position subsystem, simulation results for the backstepping NFTSM controller are shown in Figs.5—7. The tracking responses of x, y, z in Fig.5 show satisfactory tracking performances, and illustrate that the proposed strategy can accurately and effectively ensure the desired position signals. Here, the NFTSMC is compared with IBS-SMC and SMC. According to Figs.5,7, the convergence speed of NFTSMC of position tracking is relatively faster than those of IBS-SMC and SMC. Further, position errors in NFTSMC are less than that in IBS-SMC and SMC in Fig.6.

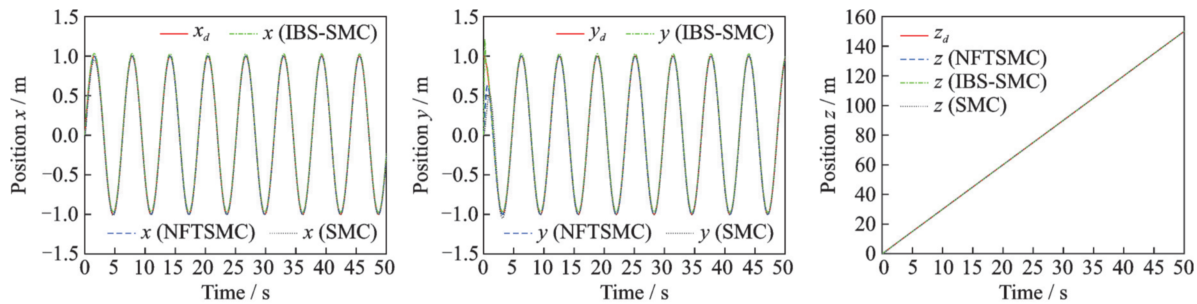

(a) x tracking (b) y tracking (c) z tracking

Fig.5 Position tracking in Scenario 1

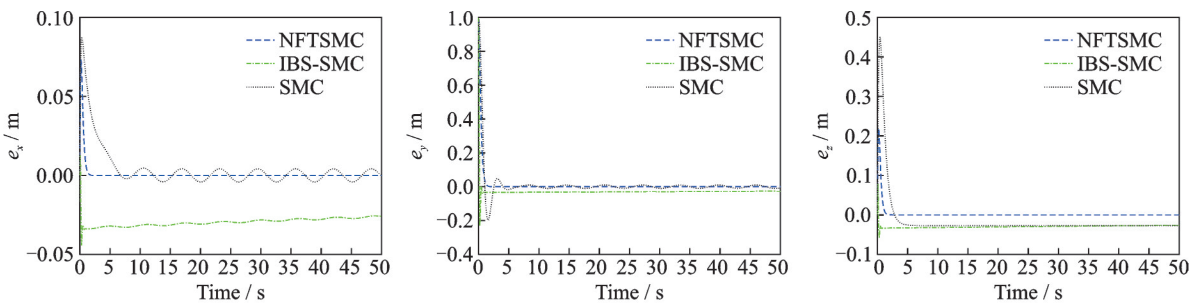

(a) x tracking error (b) y tracking error (c) z tracking error

Fig.6 Position tracking errors in Scenario 1

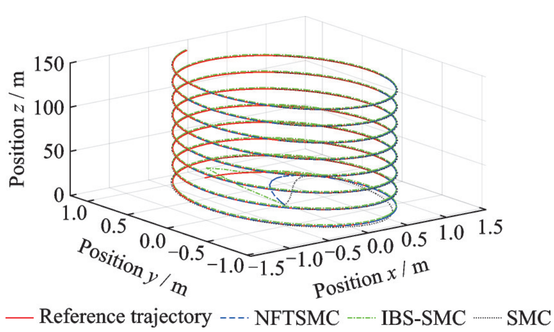

Fig.7 Position trajectory tracking in Scenario 1

4.2.2 Scenario 2: Trajectory tracking under stochastic disturbance

This scenario is set to validate the performance and characterizations of the control strategy in this paper under stochastic disturbances. The lumped uncertainties are considered as a "gust of wind" proposed in Ref.[15], then the similar form given by

$$\begin{bmatrix} d_1 \\ d_2 \\ d_3 \end{bmatrix} = \begin{bmatrix} 2.5\sin t \\ \sin(0.1t) \\ \sin(0.1t) \end{bmatrix} \text{N}\cdot\text{m}$$

$$\begin{bmatrix} d_4 \\ d_5 \\ d_6 \end{bmatrix} = \begin{bmatrix} 1.5+1.5\sin(0.5t) \\ 1.5+1.5\sin(0.5t) \\ 1.5 \end{bmatrix} \text{N}$$

The information of the compounded uncertainties in controllers comes from NDO. Fig.8 shows the lumped uncertainty estimation curves of the attitude and position subsystems. According to the simulation results, NDO can ensure that the lumped uncertainty estimates quickly and accurately converge to the actual value. When the lumped uncertainties change, NDO can still track the change trend of the upper lumped uncertainties in real time, which proves the effectiveness of NDO for the estimation of lumped uncertainties. Furthermore, the attitude tracking trajectories are given in Fig.9. The tracking responses of roll, pitch and yaw angles under the lumped uncertainty also have good tracking of the attitude reference trajectory. It is clear from Figs.10, 12 that the proposed backstepping NFTSMC con-

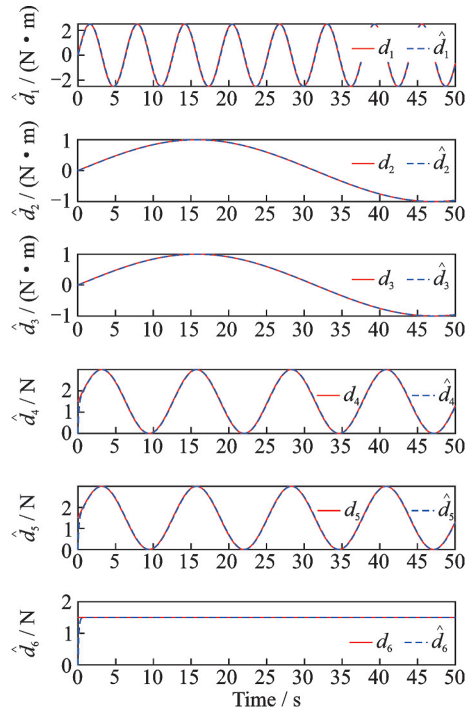

Fig.8 Estimations of the lumped uncertainties

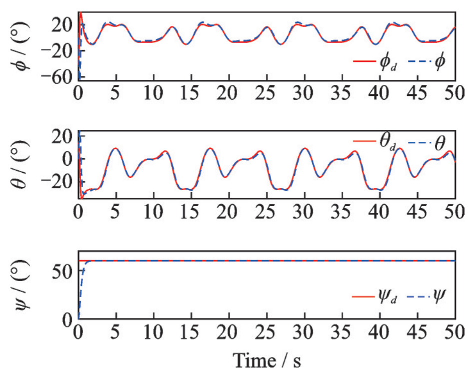

Fig.9 Attitude tracking in Scenario 2

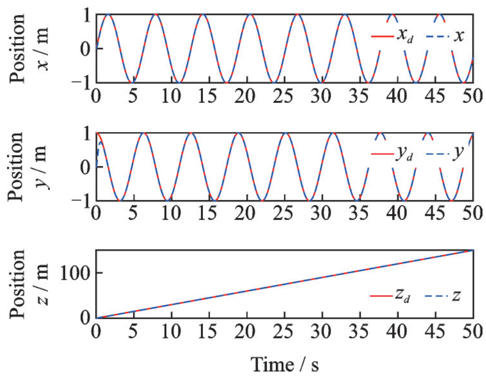

Fig.10 Position tracking in Scenario 2

troller with the quadrotor provides an excellent tracking of trajectories with a very small error of tracking. Corresponding signal inputs are depicted in Fig.11.

In Scenario 2, the proposed NFTSMC with

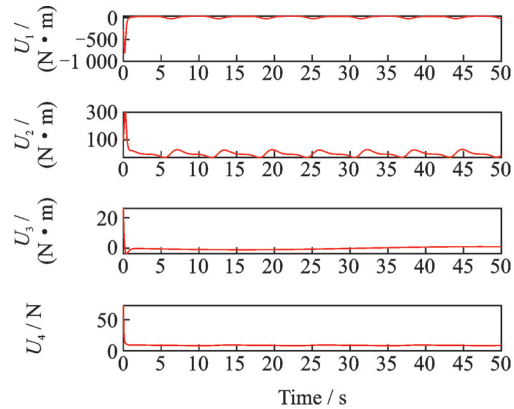

Fig.11 Control inputs in Scenario 2

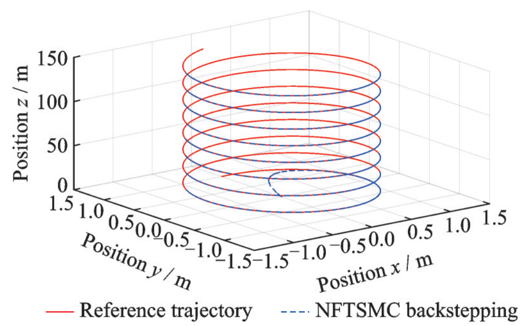

Fig.12 Position trajectory tracking in Scenario 2

reaching law for attitude subsystem and the back-stepping NFTSMC for position subsystem are able to provide a high level of accuracy and robustness against the lumped uncertainty.

4.2.3 Scenario 3: Trajectory tracking under random disturbances

In addition to the influence of stochastic disturbances considered, the influence of Gaussian random disturbances on the quadrotor dynamics is also considered in this scenario. Gaussian random disturbances are displayed in Fig.13.

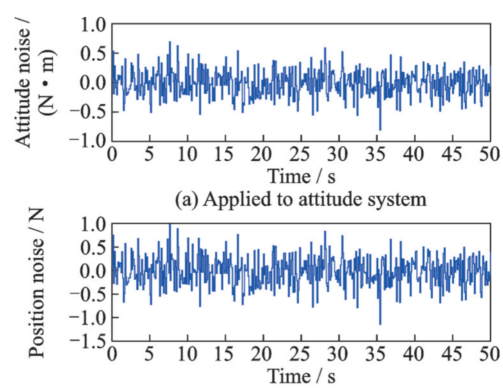

(a) Applied to attitude system

(b) Applied to position system

Fig.13 Gaussian random disturbances

The tracking performances are presented in Figs.14—16, which are shown the responses of the states and controllers with disturbances and Gaussian white noises applied. It is shown that the proposed approach demonstrates good performance. Fig.16 illustrates the trajectories of control inputs. It can be found that the NFTSM controller can track the desired signals faster even when there is random disturbance. In Fig.17, the 3D trajectories of the proposed controller are presented.

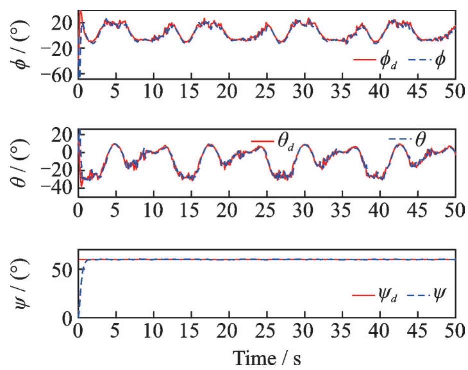
Fig.14 Attitude tracking in Scenario 3

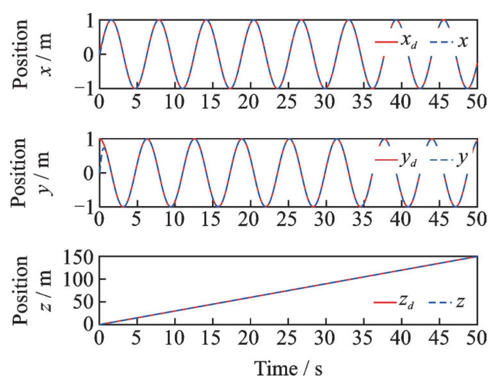
Fig.15 Position tracking in Scenario 3

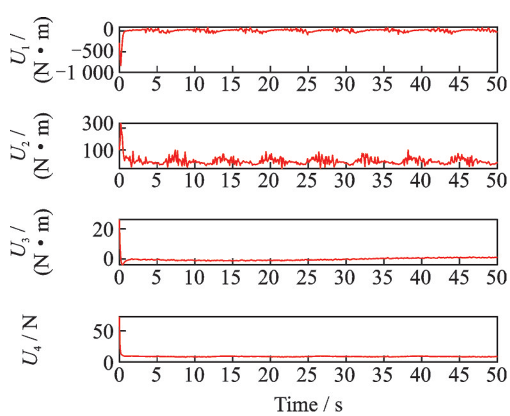
Fig.16 Control inputs in Scenario 3

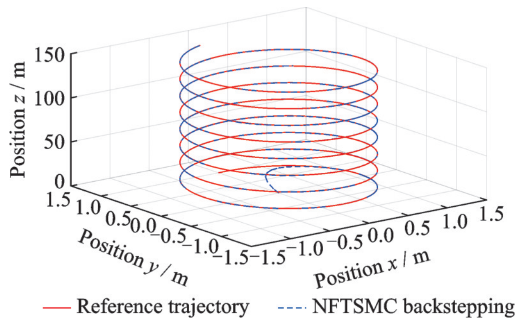

Fig.17 Position trajectory tracking in Scenario 3

5 Conclusions

A strategy of NFSMC based on a NDO is designed for quadrotors considering external disturbances and system uncertainties. A model for a quadrotor system considering the lumped uncertainty is proposed. Next, a NDO is constructed to estimate the actual values of the lumped uncertainties. Then, NFTSMC combining the reaching law is proposed for the attitude subsystem and a backstepping NFTSMC strategy is proposed for the position subsystem. The comparative study established between IBS-SMC, SMC and the proposed controller highlighted the merits of the aforementioned control schemes. Furthermore, simulation results also indicated its superior performance coping with the lumped uncertainty. Based on existing work[24-25], we will further carry out the fault prediction work for actuator faults.

References

[1] REINOSO M J, MINCHALA L I, ORTIZ P, et al. Trajectory tracking of a quadrotor using sliding mode control[J]. IEEE Latin America Transactions, 2016, 14(5): 2157-2166.

[2] BEKMEZIC I, SAHINGOZ O K, TEMEL S. Flying ad-hoc networks (FANETs): A survey[J]. Ad Hoc Networks, 2013, 11(3): 1254-1270.

[3] MENOUAR H, GUVENC I, AKKAYA K, et al. UAV-enabled intelligent transportation systems for the smart city: Applications and challenges[J]. IEEE Communications Magazine, 2017, 55(3): 22-28.

[4] GOODARZI F A, LEE D, LEE T. Geometric control of a quadrotor UAV transporting a payload connected via flexible cable[J]. International Journal of Control Automation and Systems, 2015, 13(6): 1486-1498.

[5] CHEN Fuyang, LEI Wen, ZHANG Kangkang, et al. A novel nonlinear resilient control for a quadrotor UAV via backstepping control and nonlinear disturbance observer[J]. Nonlinear Dynamics, 2016, 85(2): 1281-1295.

[6] ZHENG Enhui, XIONG Jingjing, LUO Jiliang. Second order sliding mode control for a quadrotor UAV[J]. Isa Transactions, 2014, 53(4): 1350-1356.

[7] DING Shihong, WANG Jiadian, ZHENG Weixing. Second-order sliding mode control for nonlinear uncertain systems bounded by positive functions[J]. IEEE Transactions on Industrial Electronics, 2015, 62(9): 5899-5909.

[8] DING Shihong, ZHENG Weixing, SUN Jinlin, et al. Second-order sliding mode controller design and its implementation for buck converters[J]. IEEE Transactions on Industrial Informatics, 2017, 14(5): 1990-2000.

[9] AMIN R, LI Aijun, KHAN M U, et al. An adaptive trajectory tracking control of four rotor hover vehicle using extended normalized radial basis function network[J]. Mechanical Systems and Signal Processing, 2016, 83: 53-74.

[10] KAYACAN E, MASLIM R. Type-2 fuzzy logic trajectory tracking control of quadrotor VTOL aircraft with elliptic membership functions[J]. IEEE/ASME Transactions on Mechatronics, 2016, 22(1): 339-348.

[11] MU Bingxian, ZHANG Kunku, YAN Shi. Integral sliding mode flight controller design for a quadrotor and the application in a heterogeneous multi-agent system[J]. IEEE Transactions on Industrial Electronics, 2017, 64(12): 9389-9398.

[12] WANG Haoping, YE Xunfei, TIAN Yang, et al. Model-free-based terminal SMC of quadrotor attitude and position[J]. IEEE Transactions on Aerospace and Electronic Systems, 2016, 52(5): 2519-2528.

[13] LI Shushuai, WANG Yaonan, TAN Jinhao, et al. Adaptive RBFNNs/integral sliding mode control for a quadrotor aircraft[J]. Neurocomputing, 2016, 216: 126-134.

[14] ZHANG R, QUAN Q, CAI K Y. Attitude control of a quadrotor aircraft subject to a class of time-varying disturbances[J]. IET Control Theory and Applications, 2011, 5(9): 1140-1146.

[15] NURADEEN F, MAAROUF S, HANNAH M, et al. Robust observer-based dynamic sliding mode controller for a quadrotor UAV[J]. IEEE Access, 2018, 6: 45846-45859.

[16] SHI Di, WU Zhong, CHOU Wusheng. Generalized extended state observer based high precision attitude control of quadrotor vehicles subject to wind disturbance[J]. IEEE Access, 2018, 6: 32349-32359.

[17] BENALLEGUE A, MOKHTARI A, FRIDMAN L. High-order sliding-mode observer for a quadrotor UAV[J]. International Journal of Robust and Nonlinear Control, 2008, 18(4/5): 427-440.

[18] CHEN Fuyang, JIANG Rongqiang, ZHANG Kangkang, et al. Robust backstepping sliding-mode control and observer-based fault estimation for a quadrotor UAV[J]. IEEE Transactions on Industrial Electronics, 2016, 63(8): 5044-5056.

[19] SHAO Xingling, LIU Jun, WANG Honglun. Robust back-stepping output feedback trajectory tracking for quadrotors via extended state observer and sigmoid tracking differentiator[J]. Mechanical Systems and Signal Processing, 2018, 104: 631-647.

[20] DJAMEL K, ABDELLAH M, BENALLEGUE A. Attitude optimal backstepping controller based quaternion for a UAV[J]. Mathematical Problems in Engineering, 2016, 2016(4): 1-11.

[21] WANG Ban, YU Xiang, MU Lingxia, et al. Disturbance observer-based adaptive fault-tolerant control for a quadrotor helicopter subject to parametric uncertainties and external disturbances[J]. Mechanical Systems and Signal Processing, 2019, 120: 727-743.

[22] ZHENG Shiyu, AI Xiaolin, YANG Di, et al. Integral backstepping based sliding mode trajectory tracking algorithm for quadrotor[J]. Systems Engineering and Electronics, 2019, 41(3): 643-650. (in Chinese)

[23] LIU Jinkun. Sliding mode control and MATLAB Simulation[M]. 3rd ed. Beijing: Tsinghua University Press, 2015: 34-38. (in Chinese)

[24] ZHAO Jing, DING Xiaoqian, JIANG Bin, et al. A novel control strategy for quadrotors with variable mass and external disturbance[J]. International Journal of Robust and Nonlinear Control, 2021, 31(17): 8605-8631.

[25] ZHAO Jing, WANG Xian, QIAN Juan, et al. Adaptive fault tolerant control for a quadrotor under actuator faults[C]//Proceedings of 2019 Chinese Control Conference (CCC). Guangzhou: [s.n.], 2019: 301-306.

Acknowledgements This work was supported by the National Natural Science Foundation of China (No. 52175100); the Natural Science Foundation of Jiangsu Province (No. BK20201379); the 2020 Industrial Transformation and Upgrading Project of Industry and Information Technology Department of Jiangsu Province(No.JITC-2000AX0676-71); the Natural Science Foundation of Nanjing University of Posts and

Telecommunications(No. NY221076); and the Scientific and Technological Achievements Transformation Project of Jiangsu Province (No.BA2020004).

Author Prof. ZHAO Jing received the Ph.D. degree in control theory and control engineering from Nanjing University of Aeronautics and Astronautics in 2014. She joined College of Automation, Nanjing University of Posts and Telecommunications in 2014. Her research interests include robust control, fault diagnosis, fault tolerant control and their applications in aeronautics and astronautics.

Author contributions Prof. ZHAO Jing modified the model, contributed to the data analysis, and revised the manuscript structure. Mr. WANG Peng designed the study, complied the models, conducted the analysis, interpreted the results, and wrote the manuscript. Prof. SUN Yanfei helped perform the analysis with constructive discussions. Prof. XU Fengyu and Dr. XIE Fei contributed to the discussion and background of the duty. All authors commented on the manuscript draft and approved the submission.

Competing interests The authors declare no competing interests.

(Production Editor: XU Chengting)

基于非线性干扰观测器的四旋翼非奇异快速终端滑模控制

赵 静[1,2]，王 鹏[1,2]，孙雁飞[1,2]，徐丰羽[1,2]，谢 非[3,4]

(1.南京邮电大学自动化学院/人工智能学院,南京 210023,中国;

2.南京邮电大学江苏省物联网智能机器人工程实验室,南京 210023,中国;

3.南京师范大学电气与自动化工程学院,南京 210023,中国;

4.南京中科煜宸激光技术有限公司,南京 210023,中国)

摘要：针对存在系统不确定性和外部干扰的四旋翼飞行器,提出了一种基于非线性干扰观测器(Nonlinear disturbance observer,NDO)的非奇异快速终端滑模控制(Nonsingular fast terminal sliding mode control,NFTSMC)策略。首先,利用NDO估计系统不确定性和外部干扰的实际值。然后,设计基于趋近律的NFTSM控制器用于姿态子系统(内环),该控制策略能够保证欧拉角的快速收敛以及姿态子系统的稳定性。此外,在位置子系统(外环)中采用NFTSMC与反演技术相结合的策略,保证了位置子系统的跟踪性能。最后,通过对比仿真结果表明,该方法具有更好的轨迹跟踪性能,且优于传统滑模和积分反演滑模控制的效果。

关键词：四旋翼飞行器;非线性干扰观测器;非奇异快速终端滑模控制;扰动